



A Comprehensive Review of Nusselt Number Enhancement of Natural Convection in Literal Shapes Cavities: Recent Trends and Future Challenges

Hussien Aziz Saheb^{1*}, Ahmed Kadhim Hussein²

¹ Ministry of Construction, Housing, Municipalities and Public Works, Diwaniya 00964, Iraq

² Mechanical Engineering Department, University of Babylon, College of Engineering, Hilla 00964, Iraq

Corresponding Author Email: eng419.hussien.aziz@student.uobabylon.edu.iq

Copyright: ©2025 The authors. This article is published by IETA and is licensed under the CC BY 4.0 license (<http://creativecommons.org/licenses/by/4.0/>).

<https://doi.org/10.18280/ijht.430304>

ABSTRACT

Received: 26 February 2025

Revised: 6 June 2025

Accepted: 17 June 2025

Available online: 30 June 2025

Keywords:

cavity, classical, complex geometry, enclosure, geometry, hybrid nanofluid, nanofluid, natural convection, three-dimensional, letter-shaped cavities

This research review analyzes a group of previous studies that focused on improving natural convection in literal-shaped cavities filled with base fluids (H₂O or other), nanofluids, or hybrid nanofluids. This work attempts to provide an in-depth and integrated understanding of how the complex geometry of cavities affects the boosting of heat transfer and heat exchange efficiency. Highlighting the thermophysical properties of these different fluids. The current study sought to review the most prominent engineering applications and research challenges associated with this field. This study attempts to explore recent trends in improving thermal performance through the use of unconventional fluids, and to analyze various factors such as Raleigh number (Ra), Prandtl number (Pr), Volume Fraction (ϕ), viscosity, and thermal conductivity. Numerous studies have addressed natural convection in classical cavities, whereas complex cavities (such as U, V, C, L, E, H etc.) still need further study, which constitutes a scientific gap that can be explored.

1. INTRODUCTION

One of the major disadvantages of conventional fluids is known to be low thermal conductivity and critical heat flow. Conventional fluids are water, oil, and others [1-3]. Masuda et al. [4] were the first pioneers in scientific research related to enhancing the thermal conductivity of base fluids. All studies indicate that Maxwell [5] was the first to present the idea of suspending solid nanoparticles in nanofluids to raise their thermal properties. Still, the lack of advanced technology at the time made it impossible to work with nanoparticles. researchers began conducting many different studies and researches to explore different aspects of nanofluids, Sadeghi et al. viscosity [6-8], thermal conductivity [9-11], heat transfer performance [12-14], Artificial intelligence applications for predicting various properties of nanofluids [15-17], and Engineering applications [18-20]. Many review papers summarize the most important research results of nanofluid studies in various aspects [21-23]. The particles size added to base fluids directly affects the properties of fluid, as micro particles lead to increased viscosity and increasing the drop of pressure due to their rapid settlement in the base fluid [24-26]. Choi and Eastman [27] were the first to advocate suspending solid nanoparticles in base fluids to enhance heat transfer and thermal properties. Nanoparticles ($d \leq 100$ nm) were suspended in water strengthen heat transfer through improving thermal conductivity in base fluids. Three mechanisms of heat transfer in fluids: free, forced, and mixed convection [28, 29]. Dahani et al. [28] found that the use of a (water/Ag) in a square cavity improved heat transfer. Chen et al. [30] concluded that suspending the nanoparticles in the base fluid, a slight change

in the streamline of free convection and contours of temperature, these changes are more noticeable for forced convection. Sheikholeslami et al. [31] examined the thermophoresis and Brownian motion through a cavity filled with (alumina/water). While one of them studied effect of porous cavity medium on Nu number [32].

Nowadays, complex geometries cavities have become interesting and a focus of attention in various industries such as renewable energy, HVAC, Cooling equipment, solar collectors and electronic devices. The cavity geometry was considered one of the important parameters related to enhancing heat transfer through the cavities, as different shapes were used rectangular, triangular, and trapezoidal cavity [33-35], Sun and Pop [36] used three types of nanoparticles to investigate characteristics of temperature and Nu in a porous triangular cavity.

Many researches and studies were conducted and dealt with many parameters and boundary conditions to demonstrate how to elevate heat transfer, such as focus on the effect of a wavy wall [37], heat generation [36], heat flux [37], and wall temperature [38].

Al-Zamily [40] conducted a numerical study to investigate the influence of a uniform magnetic field on natural convection within a semi-circular cavity filled with Cu–water nanofluid under partial heat flux conditions. The findings revealed that the heat transfer rate increases with higher (Ra) and greater nanoparticle volume fractions, whereas it decreases as the (Ha) increases.

Hatami et al. [39] examined natural convection in a wavy cavity. Cosine function was presumed for the inner wall equation, the heat transfer and Nu increased rapidly. Many

modern technologies, such as nuclear reactors, highlight the importance of nanofluids with magnetic fields in various cavities [41]. Nemati et al. [42] evaluated the effect of magnetic field on natural convection through a rectangular cavity. They concluded that increasing the magnetic field intensity reduces the rate of heat transfer in the cavity. Various numerical methods, including (FDM), (FVM) and (FEM) methods were used to solve various problems of natural convection [8]. The important prediction tool used to solve natural convection problems is the Lattice Boltzmann method (LBM) [43, 44]. Sheikholeslami et al. [45] used LBM and a cylindrical cavity to study the natural convection. Natural convection in a wavy circular cavity was examined by Hatami [46]. Triangular cavities as well as 3D Regular Shape Enclosures were excluded because they were previously addressed in the research of Ghoben and Hussein [47, 48]. Walker and Homsy [49] investigated the effect of the (Da) on the (Nu) by analyzing the natural convection in a porous cavity. The basic idea of this research review is to provide a comprehensive review of studies conducted on natural convection in letter-shaped cavities (H-E-I-C-L, and U). This review provides very important information about the methods and techniques used recently. It also presents a comprehensive overview of both strengths and weaknesses, and most importantly, the amazing results of studies conducted in this field. Although many experimental and numerical studies have been conducted to review the mixed and forced convection of nanofluids in cavities, no one has studied the overview of natural convection of nanofluids in letter-shaped cavities. In the following sections, the literature on natural convection of nanofluids in literal shapes cavities will be presented and discussed. Moreover, the general trend of research papers published in recent years will be presented, addressing the most commonly used nanoparticles, in order to provide a clear view and give a comprehensive idea of the studies carried out in this specialized field. According to the works examined in this review, there are a limited number of studies in the scientific literature that have been conducted to investigate the natural convection of nanofluids in letter-shaped cavities. On the other hand, there is only little research, most of which focused on mixed or forced convection, while natural convection has not been adequately addressed. This review has highlighted a scarcity of experimental studies on natural convection in geometrically literal cavities, emphasizing the need for practical implementation to better understand its behavior and demonstrate its significance across various engineering applications. It is worth noting that the majority of the studies reviewed herein are limited to laminar flow conditions. Consequently, there exists a significant research gap in exploring transitional and turbulent regimes, which are crucial for accurately modeling real-world thermal systems and enhancing the reliability of numerical predictions. In the next section (2), the literal-shaped cavities are discussed and divided into five categories based on the shapes of the cavities.

2. CAVITIES WITH LITERAL SHAPES, THEIR TYPES AND THEIR IMPORTANCE

Letter-shaped cavities are geometric structures shaped like letters of the alphabet (such as H, L, T, U, C, E) and are used to improve natural convection in thermal applications. The design of these cavities differs from classical cavities (rectangular, square, circular), as the literal design allows

better control of fluid flow and improved heat distribution within the cavity. literal-shaped cavities can be classified based on their geometric shape and the way the fluid flows inside them.

2.1 H-shape cavities

Keramat et al. [50] used single-phase model to solve natural convection in a H-cavity with V-shaped baffle. They studied the effect of (AR, ϕ , and Ra) on Nu, as shown in the Figure 1, The baffle position affects Nu , the top baffle reduces heat transfer, while the bottom baffle increases heat transfer. Additionally, a non-adiabatic baffle improves heat transfer more than an insulated baffle in the H cavity.

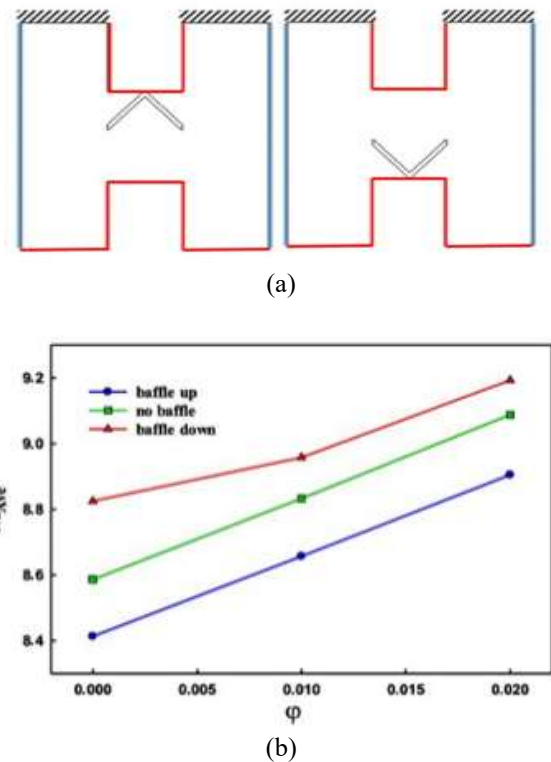


Figure 1. (a) Cavity geometry, (b) Baffle effect on Nu [50]

Keramat et al. [51] studied the free convection in an H-cavity with six porous inclined fins as shown in Figure 2(a). This study was conducted numerically by examining several key parameters Ra (10^3 – 10^5), porosity ($\epsilon=0$ – 1), AR (0.1, 0.2) Da (10^{-10} – 10^{-2}), and angle of fin (68° , 90° , 112°). They found that the max heat transfer was at $\alpha=90^\circ$ and AR=0.2, with a 60% increase in Nu for the porous fins. At low Da level ($<10^{-6}$), the porous fins are found to be like solid fins, while high Ra and porosity improved heat transfer as shown in Figure 2(b).

Loukili et al. [52] used (GFEM) to analyze natural convection in an H-cavity as shown in Figure 3(a). The cavity is filled with air. Important parameters include the (Ra= 10 – 10^6) and ratio of internal height (0%, 50%, 85%). This research found that increasing Ra enhanced heat transfer and generated multiple vortices, while higher internal height ratio reduces flow of fluid and weakens heat transfer. (Nu) increased and reaching its peak at Ra= 10^6 due to enhanced natural convection. In contrast, increasing the internal height ratio reduces Nu by restricting flow of fluid. The max heat transfer condition occurs at Ra= 10^6 with 0% internal height ratio, as illustrated in Figure 3(b).

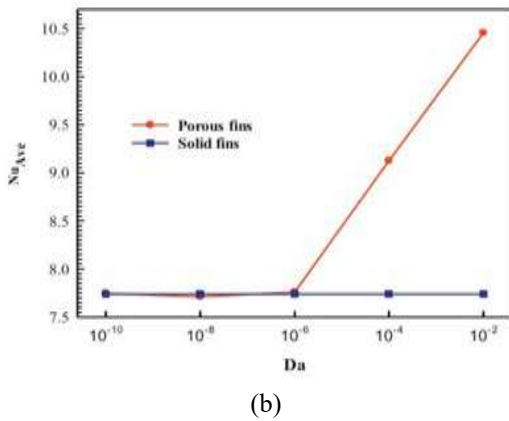
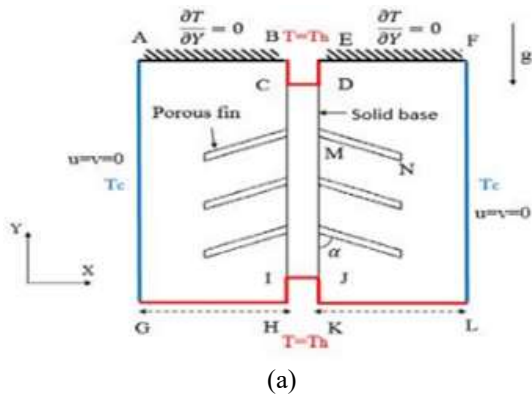


Figure 2. (a) Cavity geometry, (b) Porous fin effect on \bar{Nu} [51]

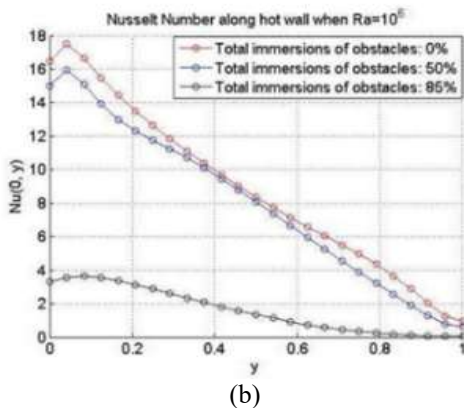
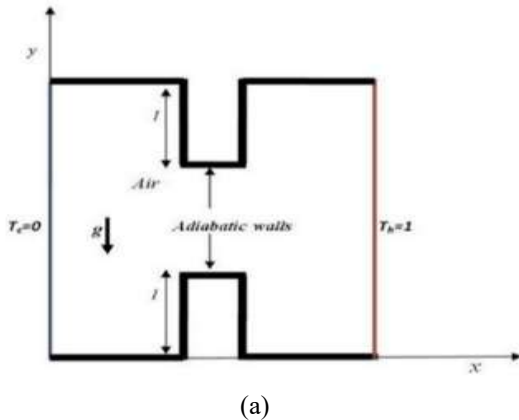


Figure 3. (a) Cavity geometry [52], (b) The effect of height aspects on the local (Nu)

Nadeem et al. [53] used the (GFEM) to simulate natural

convection. Figure 4(a) shows H-cavity filled with (Cu–Al₂O₃–H₂O). The main parameters analyzed include ($Ra=10^3-10^6$), ($AR=0.1-0.4$), Casson parameter ($\gamma=0.1-2$), and ($\phi=0.005-0.020$). Results indicate that increasing Ra , γ , and ϕ enhances heat transfer, while a higher (AR) reduces (\bar{Nu}). The optimal heat transfer is achieved at $\eta=0.1$, $Ra=10^6$, and $\phi=0.020$, where the convective effects are maximized. Max heat transfer at $AR=0.1$ and $AR=2$, where (\bar{Nu}) reaches its highest value. Increasing AR reduces heat transfer, while increasing γ improves thermal flow by lowering viscosity and enhancing natural convection as shown in Figure 4(b).

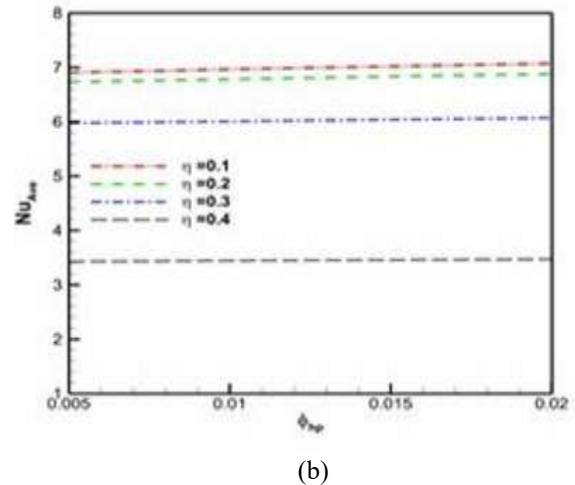
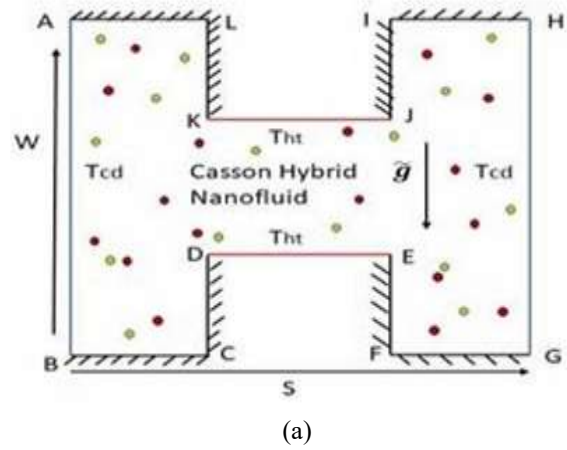


Figure 4. (a) Cavity geometry [53], (b) The effect of (ϕ and AR) on \bar{Nu} [53]

Rahimi et al. [54] studied the natural convection in an H-cavity filled with SiO₂/TiO₂/H₂O-EG as shown in Figure 5(a), this study used a numerical method (LBM) with entropy generation analysis. The basic parameters in this numerical research included: ($Ra=10^3-10^6$), ($\phi=0.5\%-3\%$), aspect ratio variations, and internal body arrangements. The results of this study as show in Figure 5(b) at higher Ra enhances heat transfer due to stronger convection, while a higher (ϕ) enhanced thermal conductivity, leading to a higher Nu . However, an increase in the (AR) tends to suppress the overall convective performance, resulting in a lower (Nu) due to constrained flow circulation. Conversely, optimal heat transfer enhancement is achieved under conditions of high (Ra) and elevated (ϕ), where buoyancy-driven convection is dominant and thermal transport is significantly intensified.

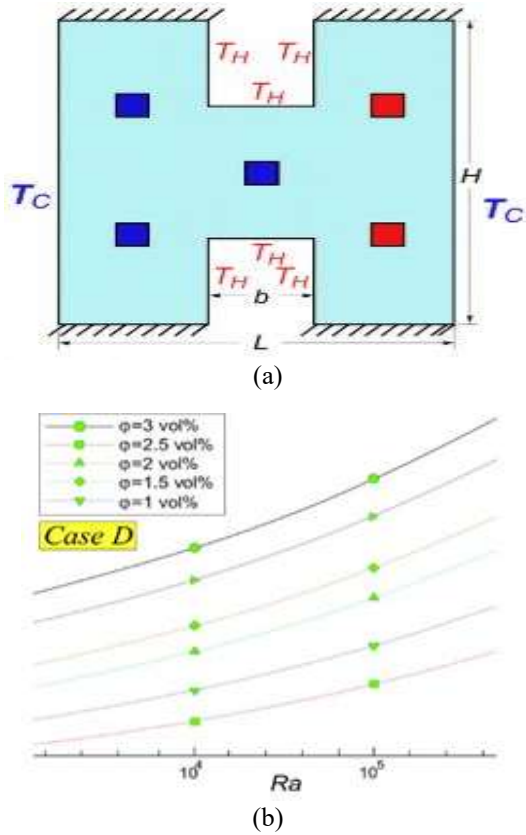


Figure 5. (a) Cavity geometry, (b) The effect of (Ra , ϕ) on \overline{Nu} [54]

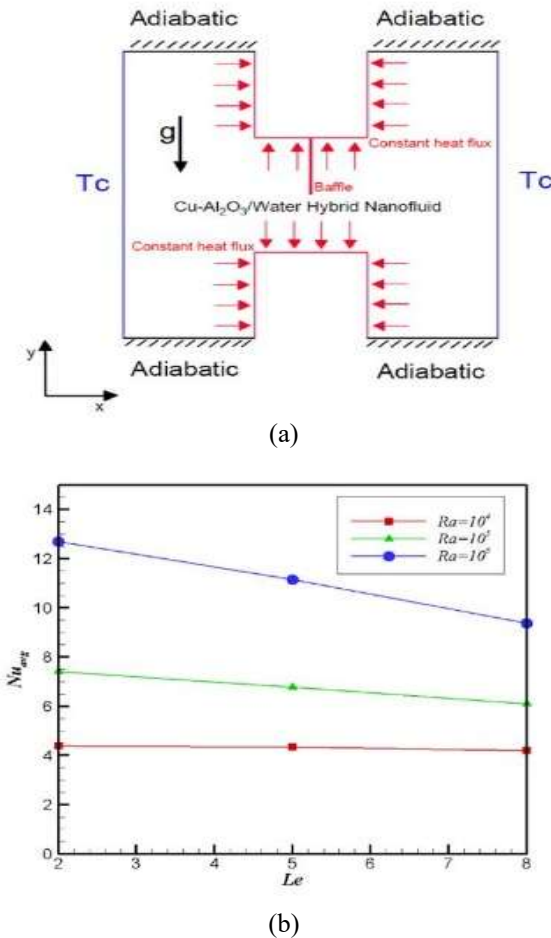


Figure 6. (a) Cavity geometry, (b) The effect of Ra and Le on \overline{Nu} ($N=3$) [55]

Eshaghi et al. [55] studied double diffusive natural convection in an H-cavity with a corrugated wall and baffle (Figure 6(a)). A hybrid nanofluid was simulated ($Cu/Al_2O_3/H_2O$). Main parameters examined included ($Ra=10^4 - 10^6$), baffle inclination angle (-60° to $+60^\circ$), Lewis number ($Le=2-8$), Buoyancy ratio ($N=1-3$), and ($AR=0.375-1.5$). This study reached with an increase in the Ra and N , heat transfer is enhanced, while in the case of an increase in Le , the \overline{Nu} and Sh_{avg} decrease. The optimal configuration for maximum heat transfer is at $\theta=-60^\circ$ without corrugation, while $\theta=+60^\circ$ without corrugation gives the optimal performance of mass transfer. Figure 6(b) presents the impact of (Ra), (Le), and buoyancy ratio (N) on both heat and mass transfer within the H-shaped cavity. The (\overline{Nu}) and (Sh_{avg}) increase with higher values of Ra and N , indicating enhanced convection due to stronger buoyancy forces. In contrast, increasing the Lewis number (Le) leads to a decrease in both \overline{Nu} and Sh_{avg} , as higher Le suppresses thermal and mass diffusion. The most efficient heat transfer performance is achieved at $Ra=10^6$ and $N=3$, while elevated Le values are associated with reduced overall transfer efficiency.

2.2 L-shape cavity

Saleem et al. [56] examined natural convection under a time-periodic temperature boundary and field of magnetic in an L-cavity filled with Cu/H_2O as show in Figure 7(a). they used ($10^3 \leq Ra \leq 10^8$), ($0 \leq Ha \leq 100$), ($0 \leq \phi \leq 0.2$), ($0.2 \leq AR \leq 0.8$), ($0 \leq f \leq 100$), and ($0 \leq A \leq 2$). This study found that as the Ra decreases, conduction dominates, while as the Ra increases, the effect of convection increases. Increasing Ha suppresses convection, reducing heat transfer, however nanofluid improved it, particularly at low Ha . The ideal heat transfer occurs at $AR=0.2$, with best temperature oscillation at $f \approx 6$. Figure 7(b) showed that the thermal oscillation will improve the natural convection, the value of Nu^* increases with frequency (f), and reaches its highest value at $f \approx 6$ before it decreases. This happens due to improved fluid circulation, which leads to enhanced heat transfer. At low frequencies the effect is minimal, while at the optimal frequency the oscillations will correspond to the movement of the fluid, and thus efficiency will increase, while at higher frequencies viscous forces lead to reduced efficiency.

Suchana et al. [57] investigated natural convection in an L-cavity, and used $MWCNTs/H_2O$ as shown in Figure 8(a). This study adopted a numerical model the Multiple-Relaxation-Time (LBM). key parameters, including ($3 \times 10^3 \leq Ra \leq 3 \times 10^5$), ($0.0 \leq \phi \leq 0.01$), Buoyancy ratio ($-2 \leq Br \leq 2$), Soret number ($0.0 \leq Sr \leq 0.2$), and Dufour number ($0.0 \leq Df \leq 0.2$). The results of this research demonstrated that increasing Ra , ϕ , and Sr improves mass and heat transfer (Nu and Sh increase) as shown in Figure 8(b), max Nu at $Ra=3 \times 10^5$. A higher ϕ enhanced thermal conductivity, leading to an increase in local Nu , but reduces local (Sh). Furthermore, entropy generation rises with Ra , while the Bejan number remains constant.

Nia et al. [58] analyzed natural convection of $Cu-H_2O$ in a baffled L-cavity. They examined the effects of ($10^3 \leq Ra \leq 10^5$), ($0 \leq \phi \leq 0.05$), and baffle configurations length ($15 \leq L \leq 30$) cm, position $S=40$ cm, 60 cm. Results of this study showed that at low Ra (10^3-10^4), a baffle always improves heat transfer, Whereas at high Ra (10^5), only a long baffle ($L=30$ cm) enhanced convection. Figure 9(a) showed the geometry of cavity while (9-b) shows the best performance is achieved with case C ($L=30$ cm, $S=40$ cm), which maximizes (Nu), making it the optimal design for efficient management of heat transfer.

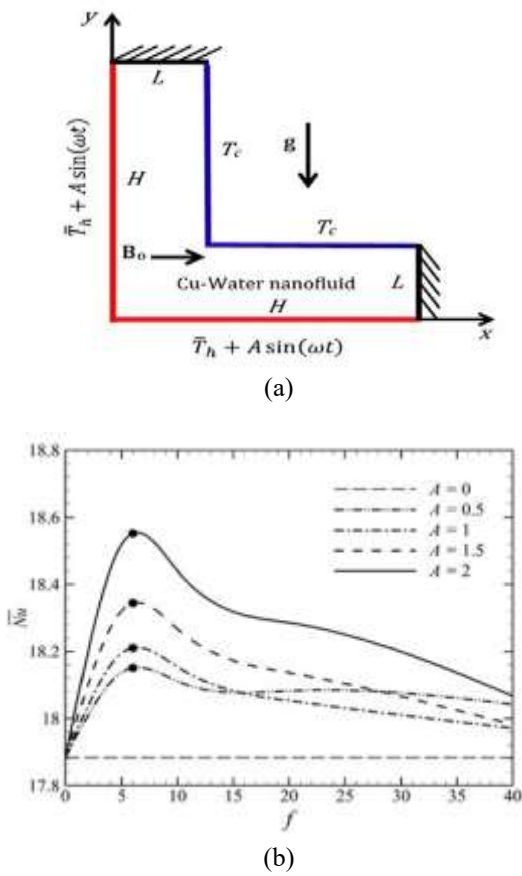


Figure 7. (a) Cavity geometry [56], (b) Effect of f on \bar{Nu} [56]

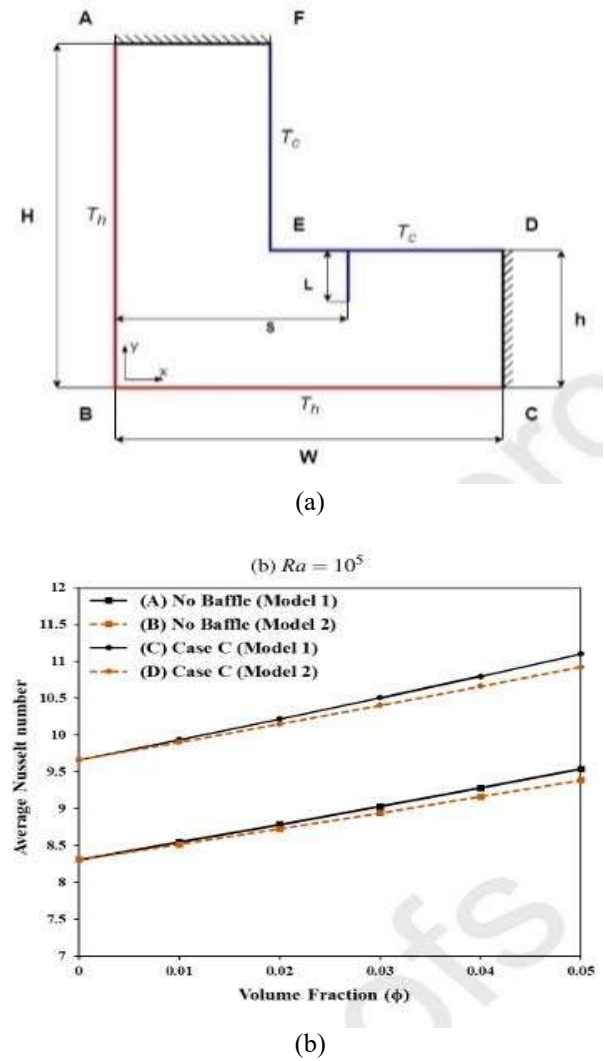


Figure 9. (a) Cavity geometry, (b) Effect of ϕ on \bar{Nu} [58]

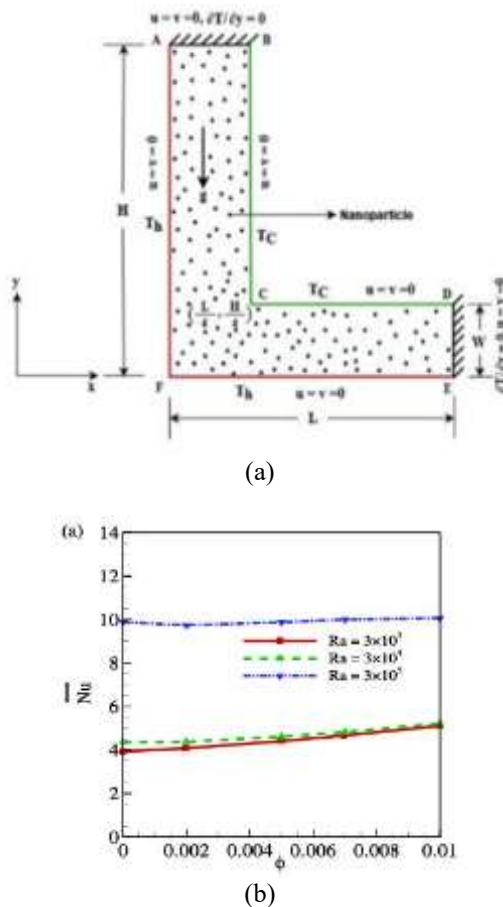


Figure 8. (a) Cavity geometry, (b) Effect of ϕ on \bar{Nu} [57]

Ghalambaz et al. [59] investigated natural convection and entropy generation in an odd-shaped cavity as shown in Figure 10(a), governing equations solve by (GFEM). This search analyzed the effects of (Ra) , (ϕ_{hnf}) , Cu to Al_2O_3 ratio (ϕ_r) , and width ratio (WR) on \bar{Nu} . The results indicated that increased (ϕ_{hnf}) improved heat transfer when conduction is dominant but has less impact in convection regimes. The optimal configuration occurs at higher Ra and moderate WR , maximizing heat transfer efficiency. Moreover, entropy generation increases with Ra and ϕ_{hnf} , with thermal entropy dominating at low Ra and viscous entropy prevailing at high Ra . All lines are in an upward direction, indicating that the addition of nanoparticles is beneficial in all cases of this study. However, the fundamental difference is that the increase in \bar{Nu} is more significant at $Ra=10^5$ as shown in the Figure 10(b).

Mahmoodi [60] used the (FVM) and the SIMPLER algorithm to couple velocity fields and pressure to evaluated the natural convection in an L-cavity. Cu/ H_2O nanofluid in cavity as shown Figure 11(a), and. This research examined the effects of (ϕ_{hnf}) , (Ra) , and (AR) , on fluid flow and heat transfer. The results indicate that the (\bar{Nu}) increases with higher Ra and (ϕ_{hnf}) , improved heat transfer. Furthermore, the transition from conduction to convection occurs at higher (Ra) as the (AR) decreases, meaning that reducing the (AR) delays the onset of convection. Furthermore, the heat transfer rate enhanced as the (AR) decreases, making lower (AR) L-shaped cavities more effective in convective heat transfer applications.

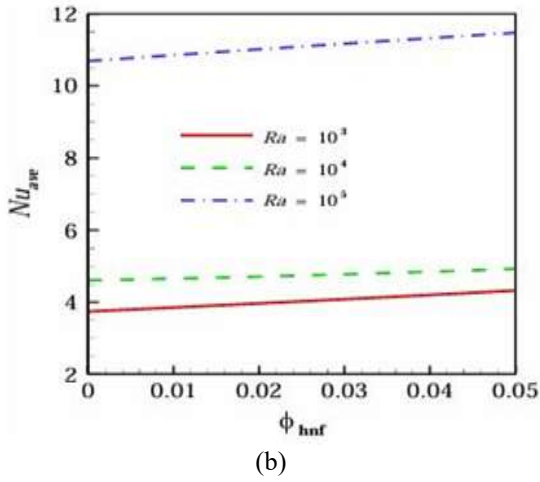
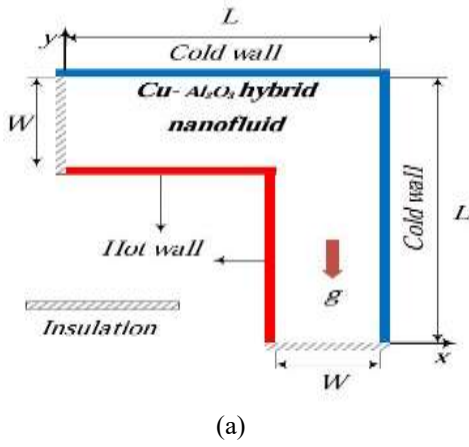


Figure 10. (a) Cavity geometry, (b) Effect of ϕ on $Nu_{\bar{a}}$ [59]

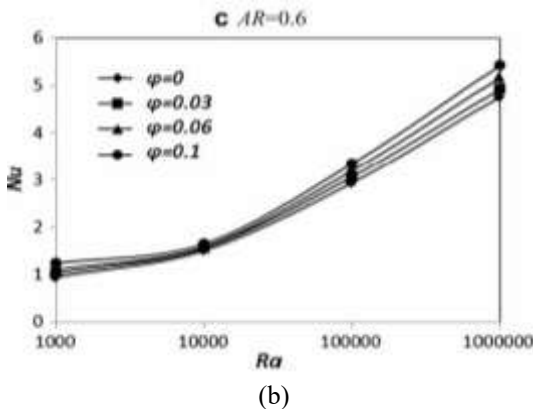
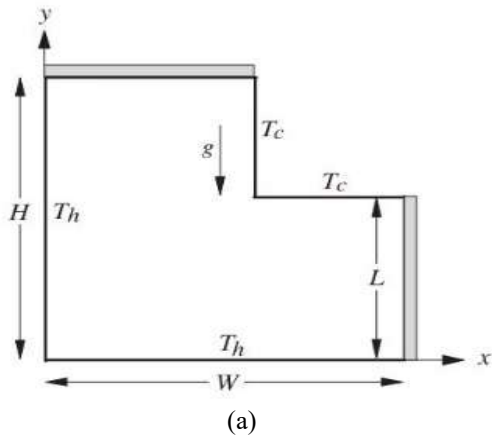


Figure 11. (a) Cavity geometry, (b) Effect of ϕ on $Nu_{\bar{a}}$ [60]

2.3 T-shape cavity

Rahman et al. [61] used semi-circular heat source to examine (MHD) in an inclined \perp -shaped cavity as shown in Figure 12(a). They used the (FEM) to analyze a micro-polar MWCNT/Fe₃O₄/H₂O. Key parameters include (Ha : 0-20), (Ra : 10^4 - 10^6), micro-rotation parameter (Γ : 0-2), and inclination of cavity (ϕ) (0° - 90°). The Results showed that higher Ha and Γ reduce the (Nu), suppressing natural convection, Whereas the highest Nu (18.876) at $Ra=10^6$, $Ha=0$, $\Gamma=0$. Increasing (ϕ) to 90° lowers Nu by 24%, and a higher micro-rotation parameter ($\Gamma=2$) reduces Nu by 27%. Figure 12 shows that $Nu_{\bar{a}}$ increases with increasing Ra and reaches its highest value at $Ra=10^6$, while it decreases with increasing Ha . $Nu_{\bar{a}}$ having the highest value at $\phi=0^\circ$ and decreasing by 24% at 90° , the use of hybrid nanofluids improved heat transfer and the highest efficiency is achieved at high Ra , low Ha and small (ϕ) as indicated (Figure 12(b)).

Askri et al. [62] examined 3D natural convection in a T-cavity. H₂O-CNT/Al₂O₃ is used. Geometry of cavity as shown in Figure 13(a), significantly affects heat transfer by modifying heat flow patterns and improved thermal performance. Increasing the size of the flanges and ribs improves buoyancy convection, increases $Nu_{\bar{a}}$ and improves heat transfer (Figure 13(b)). The (Ra) and nanoparticle concentration further amplify convection, doubling heat transfer rate at $Ra=10^6$ compared to pure H₂O. This study confirms that heat dissipation can be enhanced by changing the geometry of the cavity, which is an important factor in effective thermal management. Larger dimensions of T-cavity provided a greater heat exchange surface, optimizing efficiency of heat transfer.

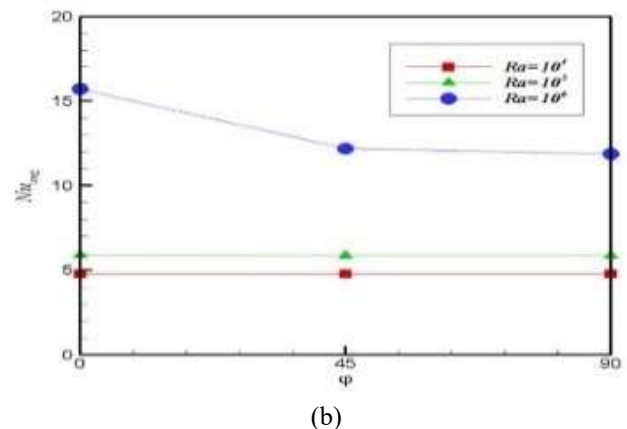
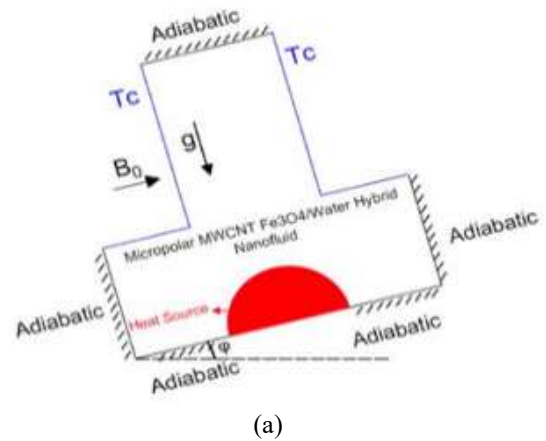


Figure 12. (a) Cavity geometry, (b) Effect of ϕ on $Nu_{\bar{a}}$ [61]

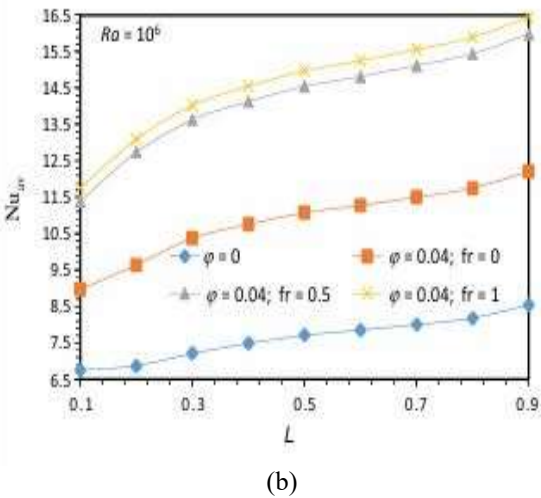
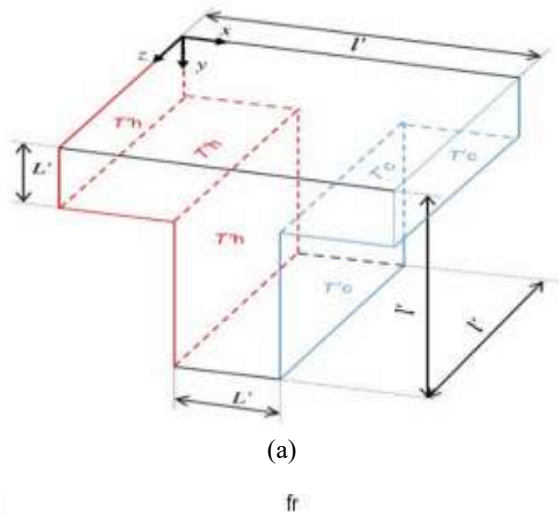


Figure 13. (a) Cavity geometry, (b) Effect of ϕ on \bar{Nu} [62]

Abu-Libdeh et al. [63] analyzed natural convection in porous cavity. Figure 14(a) shows cavity filled with hybrid nanofluid under a constant magnetic field. The geometry of cavity significantly affects performance of heat transfer by influencing circulation of fluid, vortex formation, and generation of entropy. Increasing the (Ha) suppresses convection, reducing efficiency of heat transfer. Meanwhile, the (Da) and (Ra) enhance fluid motion, enhancing convection as shown Figure 14(b). The findings confirm that cavity geometry optimizes dissipation of heat.

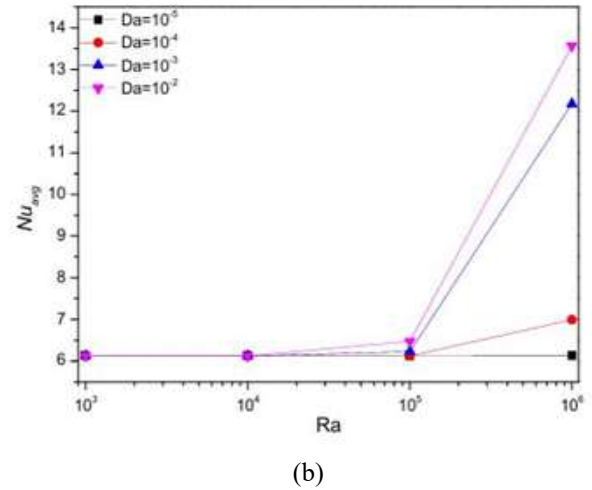
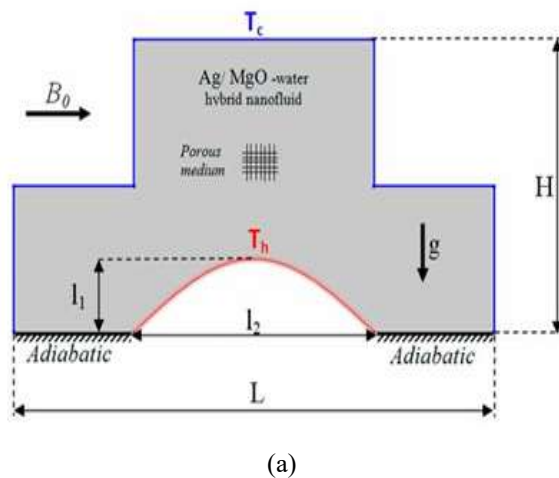


Figure 14. (a) Cavity geometry, (b) Effect of Da on \bar{Nu} [63]

2.4 U-shape cavity

Nabwey et al. [64] investigated (MHD) unsteady free convection in an inclined U-cavity as shown Figure 15(a). Cu-H₂O was the nanofluid used. The cavity adiabatic vertical walls and cooled upper horizontal walls, with a discrete heat source positioned at the bottom horizontal wall. The main parameters studied include the Ha , AR , size and position of heat source, (ϕ), and internal heat absorption/generation. Results reveal that increasing (ϕ) improves convection heat transfer, while higher (Ha) and heat source length diminish the \bar{Nu} as shown in Figure 15(b). This study indicated that convection is significantly suppressed by magnetic forces, which improved conduction within the Cu-H₂O filled U-cavity.

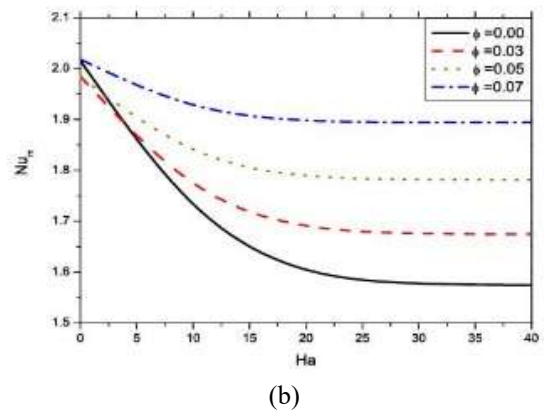
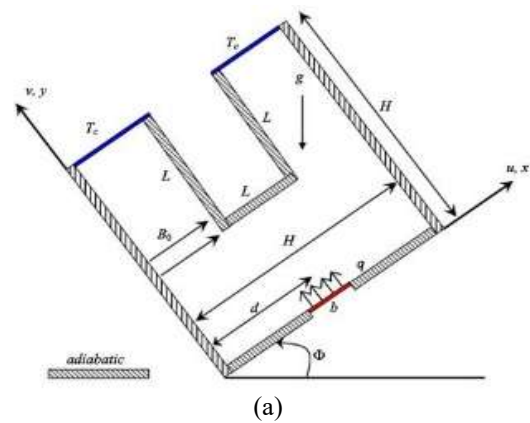
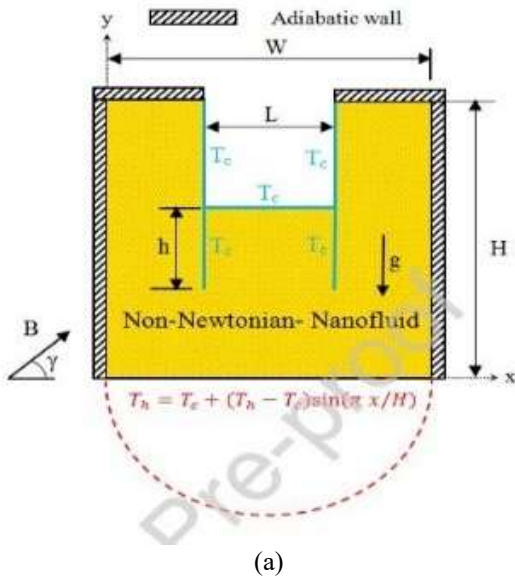
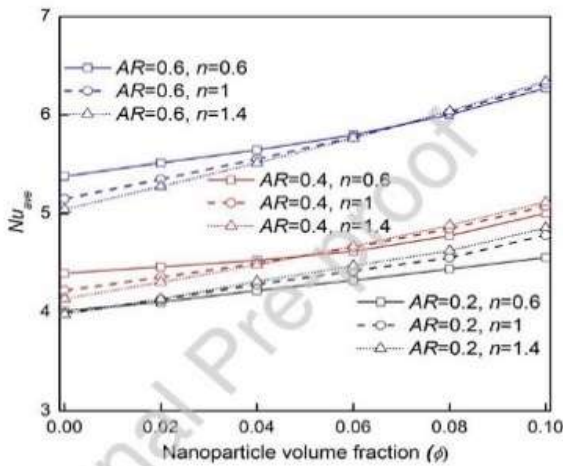


Figure 15. (a) Cavity geometry, (b) Ha effect on \bar{Nu} [64]

Ali et al. [65] utilized the (GFEM) to simulate the natural convection under a magnetic field in a U-cavity. The bottom wall was heated sinusoidally, on top is the cold baffles, and sidewalls is insulated. parameters include ($Ra=10^3-10^6$), ($Ha=0-50$), ($\phi=0.0-0.09$), ($AR=0.2-0.6$), and power law index ($0.60 \leq n \leq 1.4$). Results showed that higher Ra (10^6) and ϕ improve heat transfer, whereas $Ha > 30$ suppresses convection due to Lorentz force. Shear-thinning fluids ($n < 1$) enhanced heat transfer at $Ra=10^6$, and higher AR improves Nu by reducing thermal resistance. Figure 16(b) shows that the best result was at $AR=0.6$, $Ra=10^6$, $Ha=0$, and $\phi=0.05$.

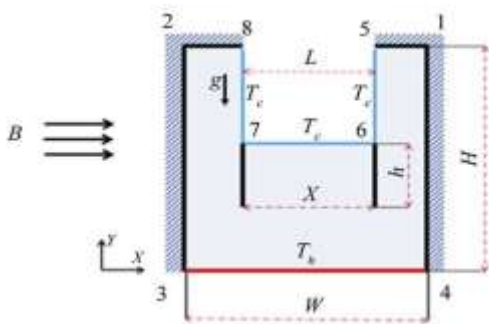


(a)



(b)

Figure 16. (a) Cavity geometry, (b) Effect of AR and ϕ on Nu [65]



(a)

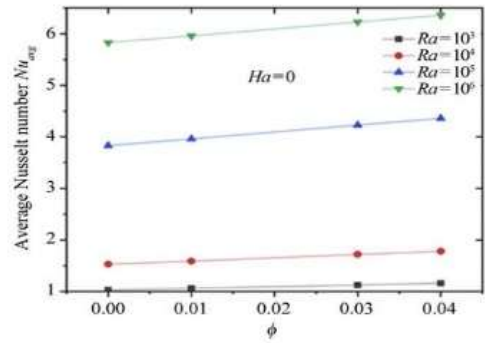
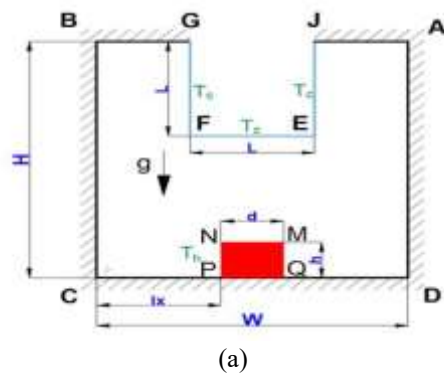


Figure 17. (a) Cavity geometry, (b) Effect of ϕ and Ha on Nu [66]

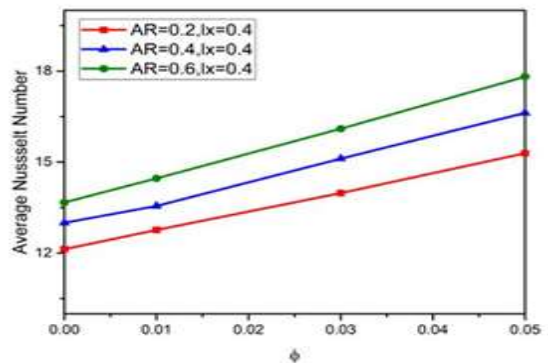
Zaim et al. [66] used the Brinkman and Wasp models to evaluate thermal conductivity of nano fluid and viscosity of nanofluid. They investigated (MHD) natural convection of Cu-H₂O in a baffled U- cavity as shown in Figure 17(a). The cavity has a cold middle baffle, insulated side walls, and heated bottom wall. parameters include ($10^3 \leq Ra \leq 10^6$), ($1 \leq Ha \leq 60$), and ($0 \leq \phi \leq 4\%$). At higher Ra and ϕ enhanced heat transfer, while $Ha > 30$ suppresses convection due to Lorentz force. Ideal conditions for heat transfer occur at, low Ha , high Ra , and increased ϕ as shown in Figure 17(b).

Ma et al. [67] studied the natural convection of Al₂O₃/H₂O and TiO₂/H₂O in a U- cavity as shown in Figure 18(a). They analyzed numerically using the (LBM) to examine the effects of ($Ra=10^3$ to 10^6), ($AR=0.2$ to 0.6), and ($\phi=0$ to 0.05) on heat transfer. Results of this research showed that increasing Ra , AR and ϕ as shown in Figure 18(b), Optimizes heat transfer, with Al₂O₃-H₂O nanofluid outperforming TiO₂-water. The increasing the hot obstacle height also improves heat transfer.



(a)

(d) $Ra = 10^6$



(b)

Figure 18. (a) Cavity geometry, (b) Effect of AR and ϕ [67]

2.5 C-E-shape cavity

Bagheri et al. [68] used (FEM) to solve natural convection in a C-cavity (Figure 19). They used the (MWCNT-Fe₃O₄-H₂O), under magnetic fields and variable heat flux. The Artificial Neural Networks with Particle Swarm Optimization is applied to Forecast the Nu. The parameters verified include (AR), (Ha), (φ), and (Ra). The (Ra) and (AR) have the effect on heat transfer, with hybrid nanofluid exceeding mono nanofluids, particularly at higher Ra values. Increasing Ha reduces efficiency of heat transfer.

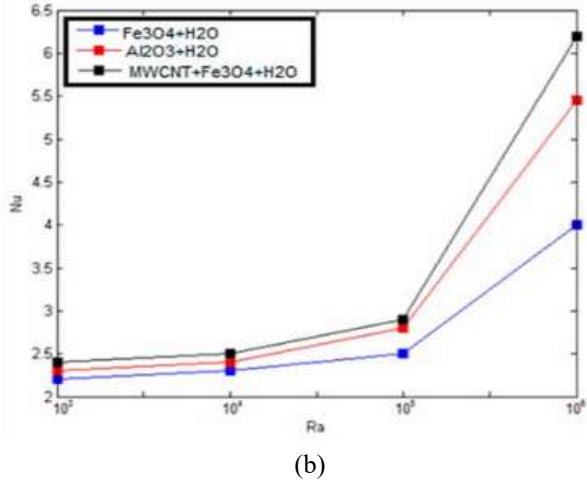
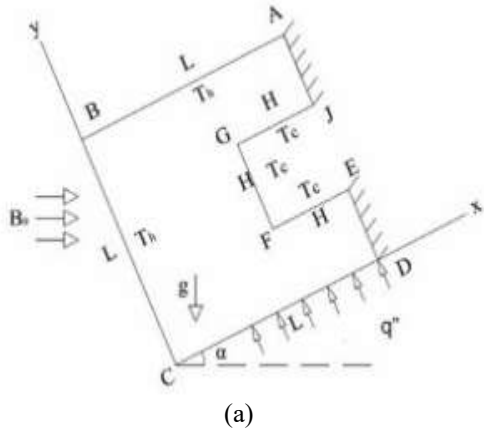
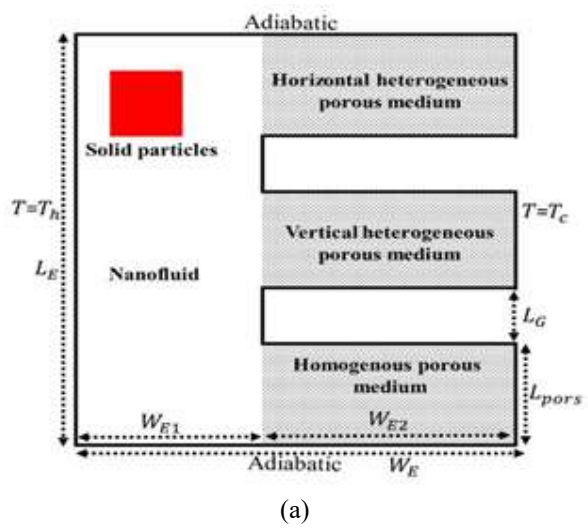
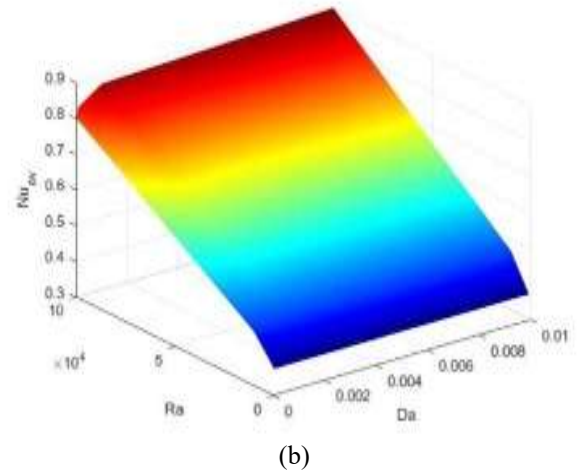


Figure 19. (a) Cavity geometry, (b) Effect of nanofluid type on Nu [68]



(a)



(b)

Figure 20. (a) Cavity geometry, (b) Effect of Ra and Da on Nu [69]

Raizah et al. [69] investigated natural convection in an E-cavity filled with Al₂O₃/H₂O as shown in Figure 20(a). This research verified the effect of heterogeneous porous media and homogeneous media, nano particles with different thermal conditions, and φ (1% to 5%) on heat transfer. Ra=10³ to 10⁵) and (Da=10⁻² to 10⁻⁵) are main parameters. Figure 20(b) showed the Nu increases with φ and Ra, with the highest Nu observed when the cavity is filled with horizontal heterogeneous porous media, boosting natural convection and thermal boundary layers.

3. MATH

The stander equations were used, and the fluid was considered water, and the flow was 3D-laminar, incompressible, and steady-state.

Governing Equations [70]

Mass conservation equation:

$$\frac{\partial u}{\partial x} + \frac{\partial v}{\partial y} + \frac{\partial w}{\partial z} = 0 \tag{1}$$

Momentum equations in the Cartesian Coordinates:

$$\rho_{nf} \left(u \frac{\partial u}{\partial x} + v \frac{\partial u}{\partial y} + w \frac{\partial u}{\partial z} \right) = -\frac{\partial P}{\partial x} + \mu_{nf} \left(\frac{\partial^2 u}{\partial x^2} + \frac{\partial^2 u}{\partial y^2} + \frac{\partial^2 u}{\partial z^2} \right) \tag{2}$$

$$\rho_{nf} \left(u \frac{\partial v}{\partial x} + v \frac{\partial v}{\partial y} + w \frac{\partial v}{\partial z} \right) = -\frac{\partial P}{\partial y} + \mu_{nf} \left(\frac{\partial^2 v}{\partial x^2} + \frac{\partial^2 v}{\partial y^2} + \frac{\partial^2 v}{\partial z^2} \right) \tag{3}$$

$$\rho_{nf} \left(u \frac{\partial w}{\partial x} + v \frac{\partial w}{\partial y} + w \frac{\partial w}{\partial z} \right) - \frac{\partial P}{\partial z} + \mu_{nf} \left(\frac{\partial^2 w}{\partial x^2} + \frac{\partial^2 w}{\partial y^2} + \frac{\partial^2 w}{\partial z^2} \right) \tag{4}$$

Table 1. Essential parameters in nanofluid studies

Physical Factor/Parameter	Effect	Equation	Applied in Governing Equations
Nanofluid Properties	Modify thermal and dynamic properties	$\rho_{nf}, \mu_{nf}, k_{nf}, C_{p,nf}$	All governing equations
Hybrid Nanofluid	Combine effects of two or more types of nanoparticles	Models for k_{hnf}, μ_{hnf}	All governing equations
(Ra)	Represents ratio of buoyancy to thermal diffusion	$Ra = (g\beta\Delta TH^3)/(\alpha\nu)$	Non-dimensional analysis
(Ha)	Quantifies magnetic field influence on flow	$Ha = B \cdot L \cdot \sqrt{(\sigma/\mu)}$	Momentum equation via Lorentz force
Porous Medium	Adds flow resistance due to porous material	$-\mu_{nf} \cdot u/K$	Momentum equation
Buoyancy Force (Boussinesq Approx.)	Represents thermal buoyancy effect	$\rho_{nf} \cdot g \cdot \beta_{nf} \cdot (T - T_0)$	Momentum equation
Lorentz Force	Represents magnetic damping effect	$-\sigma \cdot B^2 \cdot u$	Momentum equation
Thermal Boundary Conditions	Simulates realistic thermal boundaries	$T = \text{constant, or function like } \sin(x)$	Energy equation/boundary conditions

Heat transfer equation:

$$u \frac{\partial T}{\partial x} + v \frac{\partial T}{\partial y} + w \frac{\partial T}{\partial z} = \alpha_{nf} \left(\frac{\partial^2 T}{\partial x^2} + \frac{\partial^2 T}{\partial y^2} + \frac{\partial^2 T}{\partial z^2} \right) \quad (5)$$

Table 1 summarizes the main physical factors involved in numerical studies of nanofluids and hybrid nanofluids. It includes the effect of each factor, the typical equation used to model it, and the part of the governing equations where it is applied.

4. CONCLUSIONS

- i. Most of the studies conducted were numerical, and there is a scarcity of their application in reality, which gives a greater incentive to use them experimentally and benefit from them.
- ii. Classical cavities such as rectangles, squares, etc. are symmetrical and will produce uniform heat flow patterns, while complex cavities are characterized by sharp asymmetry, which leads to the generation of complex vortices and hot spots.
- iii. There is a very scarcity in verifying transitional and turbulent states, as most research has focused on the laminar state, which can make this point a scientific gap in research.
- iv. Most existing studies rely on fixed boundary conditions, which often do not reflect the real reality, leading to noticeable errors when compared with experimental results.
- v. The hybrid nanofluid is also a promising option with literal shaped cavities as it enhances heat transfer more compared to the nanofluid.
- vi. The effect of porous medium or the magnetic flux did not differ significantly from the effect in classical shaped cavities.
- vii. Cavities with sharp edges and complex angles (such as H and L) may promote the formation of thermal vortices that increase the natural convection. Efficiency.
- viii. Complex cavities provide better control over the distribution of thermal currents than conventional cavities (square and rectangular).
- ix. The H-geometric cavities with a porous medium improved the (Nu) value by an increase of 60%.
- x. Different fluids were used (water, nanofluid,

hybrid nanofluid), and no specific fluid type showed superiority in enhancing the (Nu) over the other types.

REFERENCES

- [1] Sheremet, M.A., Groşan, T., Pop, I. (2015). Steady-state free convection in right-angle porous trapezoidal cavity filled by a nanofluid: Buongiorno's mathematical model. *European Journal of Mechanics-B/Fluids*, 53: 241-250. <http://doi.org/10.1016/j.euromechflu.2015.06.003>
- [2] Asadi, A. (2018). A guideline towards easing the decision-making process in selecting an effective nanofluid as a heat transfer fluid. *Energy Conversion and Management*, 175: 1-10. <https://doi.org/10.1016/j.enconman.2018.08.101>
- [3] Asadi, A., Asadi, M., Rezaniakolaei, A., Rosendahl, L. A., Wongwises, S. (2018). An experimental and theoretical investigation on heat transfer capability of Mg(OH)₂/MWCNT-engine oil hybrid nano-lubricant adopted as a coolant and lubricant fluid. *Applied Thermal Engineering*, 129: 577-586. <https://doi.org/10.1016/j.applthermaleng.2017.10.074>
- [4] Masuda, H., Ebata, A., Teramae, K. (1993). Alteration of thermal conductivity and viscosity of liquid by dispersing ultra-fine particles. Dispersion of Al₂O₃, SiO₂ and TiO₂ ultra-fine particles. *Netsu Bussei*, 7: 227-233.
- [5] Maxwell, J. (1873). *Electricity and Magnetism*. Oxford: Clarendon Press.
- [6] Asadi, A., Alarifi, I.M., Foong, L.K. (2020). An experimental study on characterization, stability and dynamic viscosity of CuO-TiO₂/water hybrid nanofluid. *Journal of Molecular Liquids*, 307: 112987. <https://doi.org/10.1016/j.molliq.2020.112987>
- [7] Alarifi, I.M., Alkough, A.B., Ali, V., Nguyen, H.M., Asadi, A. (2019). On the rheological properties of MWCNT-TiO₂/oil hybrid nanofluid: An experimental investigation on the effects of shear rate, temperature, and solid concentration of nanoparticles. *Powder Technology*, 355: 157-162. <https://doi.org/10.1016/j.powtec.2019.07.039>
- [8] Asadi, A., Pourfatah, F. (2019). Heat transfer performance of two oil-based nanofluids containing ZnO and MgO nanoparticles; a comparative experimental investigation. *Powder Technology*, 343: 296-308. <https://doi.org/10.1016/j.powtec.2018.11.023>
- [9] Asadi, A., Alarifi, I.M., Ali, V., Nguyen, H.M. (2019).

- An experimental investigation on the effects of ultrasonication time on stability and thermal conductivity of MWCNT-water nanofluid: Finding the optimum ultrasonication time. *Ultrasonics Sonochemistry*, 58: 104639. <https://doi.org/10.1016/j.ultsonch.2019.104639>
- [10] Asadi, A., Asadi, M., Siahmargoi, M., Asadi, T., Andarati, M.G. (2017). The effect of surfactant and sonication time on the stability and thermal conductivity of water-based nanofluid containing Mg(OH)₂ nanoparticles: An experimental investigation. *International Journal of Heat and Mass Transfer*, 108: 191-198. <https://doi.org/10.1016/j.ijheatmasstransfer.2016.12.022>
- [11] Esfe, M.H., Wongwises, S., Naderi, A., Asadi, A., Safaei, M.R., Rostamian, H., Dahari, M., Karimipour, A. (2015). Thermal conductivity of Cu/TiO₂-water/EG hybrid nanofluid: Experimental data and modeling using artificial neural network and correlation. *International Communications in Heat and Mass Transfer*, 66: 100-104. <https://doi.org/10.1016/j.icheatmasstransfer.2015.05.014>
- [12] Alshayji, A., Asadi, A., Alarifi, I.M. (2020). On the heat transfer effectiveness and pumping power assessment of a diamond-water nanofluid based on thermophysical properties: An experimental study. *Powder Technology*, 373: 397-410. <https://doi.org/10.1016/j.powtec.2020.06.068>
- [13] Asadi, A., Asadi, M., Rezaniakolaei, A., Rosendahl, L.A., Afrand, M., Wongwises, S. (2018). Heat transfer efficiency of Al₂O₃-MWCNT/thermal oil hybrid nanofluid as a cooling fluid in thermal and energy management applications: An experimental and theoretical investigation. *International Journal of Heat and Mass Transfer*, 117: 474-486. <https://doi.org/10.1016/j.ijheatmasstransfer.2017.10.036>
- [14] Alnaqi, A.A., Aghakhani, S., Pordanjani, A.H., Bakhtiari, R., Asadi, A., Tran, M.D. (2019). Effects of magnetic field on the convective heat transfer rate and entropy generation of a nanofluid in an inclined square cavity equipped with a conductor fin: Considering the radiation effect. *International Journal of Heat and Mass Transfer*, 133: 256-267. <https://doi.org/10.1016/j.ijheatmasstransfer.2018.12.110>
- [15] Asadi, A., Bakhtiyari, A.N., Alarifi, I.M. (2021). Predictability evaluation of support vector regression methods for thermophysical properties, heat transfer performance, and pumping power estimation of MWCNT/ZnO-engine oil hybrid nanofluid. *Engineering with Computers*, 37(4): 3813-3823. <https://doi.org/10.1007/s00366-020-01038-3>
- [16] Asadi, A., Alarifi, I.M., Nguyen, H.M., Moayedi, H. (2021). Feasibility of least-square support vector machine in predicting the effects of shear rate on the rheological properties and pumping power of MWCNT-MgO/oil hybrid nanofluid based on experimental data. *Journal of Thermal Analysis and Calorimetry*, 143: 1439-1454. <https://doi.org/10.1007/s10973-020-09279-6>
- [17] Alarifi, I.M., Nguyen, H.M., Naderi Bakhtiyari, A., Asadi, A. (2019). Feasibility of ANFIS-PSO and ANFIS-GA models in predicting thermophysical properties of Al₂O₃-MWCNT/oil hybrid nanofluid. *Materials*, 12(21): 3628. <https://doi.org/10.3390/ma12213628>
- [18] Pourfattah, F., Sabzpooshani, M., Toghraie, D., Asadi, A. (2021). On the optimization of a vertical twisted tape arrangement in a channel subjected to MWCNT-water nanofluid by coupling numerical simulation and genetic algorithm. *Journal of Thermal Analysis and Calorimetry*, 144: 189-201. <https://doi.org/10.1007/s10973-020-09490-5>
- [19] Lyu, Z., Pourfattah, F., Arani, A.A.A., Asadi, A., Foong, L.K. (2020). On the thermal performance of a fractal microchannel subjected to water and kerosene carbon nanotube nanofluid. *Scientific Reports*, 10(1): 7243. <https://doi.org/10.1038/s41598-020-64142-w>
- [20] Lyu, Z., Asadi, A., Alarifi, I.M., Ali, V., Foong, L.K. (2020). Thermal and fluid dynamics performance of MWCNT-water nanofluid based on thermophysical properties: An experimental and theoretical study. *Scientific Reports*, 10(1): 5185. <https://doi.org/10.1038/s41598-020-62143-3>
- [21] Asadi, A., Aberoumand, S., Moradikazerouni, A., Pourfattah, F., Żyła, G., Estellé, P., Mahian, O., Wongwises, S., Nguyen, H.M., Arabkoohsar, A. (2019). Recent advances in preparation methods and thermophysical properties of oil-based nanofluids: A state-of-the-art review. *Powder Technology*, 352: 209-226. <https://doi.org/10.1016/j.powtec.2019.04.054>
- [22] Asadi, A., Pourfattah, F., Szilágyi, I.M., Afrand, M., Żyła, G., Ahn, H.S., Wongwises, S., Nguyen, H.M., Arabkoohsar, A., Mahian, O. (2019). Effect of sonication characteristics on stability, thermophysical properties, and heat transfer of nanofluids: A comprehensive review. *Ultrasonics Sonochemistry*, 58: 104701. <https://doi.org/10.1016/j.ultsonch.2019.104701>
- [23] Arshad, A., Jabbar, M., Yan, Y., Reay, D. (2019). A review on graphene based nanofluids: Preparation, characterization and applications. *Journal of Molecular Liquids*, 279: 444-484. <https://doi.org/10.1016/j.molliq.2019.01.153>
- [24] Khanafer, K., Vafai, K., Lightstone, M. (2003). Buoyancy-driven heat transfer enhancement in a two-dimensional enclosure utilizing nanofluids. *International Journal of Heat and Mass Transfer*, 46(19): 3639-3653. [https://doi.org/10.1016/S0017-9310\(03\)00156-X](https://doi.org/10.1016/S0017-9310(03)00156-X)
- [25] Asadi, A., Asadi, M., Rezaei, M., Siahmargoi, M., Asadi, F. (2016). The effect of temperature and solid concentration on dynamic viscosity of MWCNT/MgO (20-80)-SAE50 hybrid nano-lubricant and proposing a new correlation: An experimental study. *International Communications in Heat and Mass Transfer*, 78: 48-53. <https://doi.org/10.1016/j.icheatmasstransfer.2016.08.021>
- [26] Asadi, M., Asadi, A. (2016). Dynamic viscosity of MWCNT/ZnO-engine oil hybrid nanofluid: An experimental investigation and new correlation in different temperatures and solid concentrations. *International Communications in Heat and Mass Transfer*, 76: 41-45. <https://doi.org/10.1016/j.icheatmasstransfer.2016.05.019>
- [27] Choi, S.U., Eastman, J.A. (1995). Enhancing thermal conductivity of fluids with nanoparticles. Argonne National Lab.(ANL), Argonne, IL (United States), No. ANL/MSD/CP-84938; CONF-951135-29.
- [28] Dahani, Y., Hasnaoui, M., Amahmid, A., Hasnaoui, S. (2017). Lattice-Boltzmann modeling of forced convection in a lid-driven square cavity filled with a nanofluid and containing a horizontal thin heater. *Energy*

- Procedia, 139: 134-139.
<https://doi.org/10.1016/j.egypro.2017.11.186>
- [29] Esmacili, H., Armaghani, T., Abedini, A., Pop, I. (2019). Turbulent combined forced and natural convection of nanofluid in a 3D rectangular channel using two-phase model approach. *Journal of Thermal Analysis and Calorimetry*, 135: 3247-3257.
<https://doi.org/10.1007/s10973-018-7471-9>
- [30] Chen, C.L., Chang, S.C., Chang, C.K. (2015). Lattice Boltzmann simulation for mixed convection of nanofluids in a square enclosure. *Applied Mathematical Modelling*, 39(8): 2436-2451.
<https://doi.org/10.1016/j.apm.2014.10.049>
- [31] Sheikholeslami, M., Gorji-Bandpy, M., Ganji, D.D., Rana, P., Soleimani, S. (2014). Magnetohydrodynamic free convection of Al₂O₃-water nanofluid considering Thermophoresis and Brownian motion effects. *Computers & Fluids*, 94: 147-160.
<https://doi.org/10.1016/j.compfluid.2014.01.036>
- [32] Hoseinpour, B., Ashorynejad, H.R., Javaherdeh, K. (2017). Entropy generation of nanofluid in a porous cavity by lattice Boltzmann method. *Journal of Thermophysics and Heat Transfer*, 31(1): 20-27.
<https://doi.org/10.2514/1.T4652>
- [33] Mamun, M.A.H., Tanim, T.R., Rahman, M.M., Saidur, R., Nagata, S. (2011). Analysis of mixed convection in a lid driven trapezoidal cavity. *Convection and Conduction Heat Transfer*, 55-82. <http://doi.org/10.5772/21108>
- [34] Saha, S.C. (2011). Scaling of free convection heat transfer in a triangular cavity for Pr>1. *Energy and Buildings*, 43(10): 2908-2917.
<https://doi.org/10.1016/j.enbuild.2011.07.016>
- [35] Saleh, H., Roslan, R., Hashim, I. (2011). Natural convection heat transfer in a nanofluid-filled trapezoidal enclosure. *International Journal of Heat and Mass Transfer*, 54(1-3): 194-201.
<https://doi.org/10.1016/j.ijheatmasstransfer.2010.09.053>
- [36] Sun, Q., Pop, I. (2011). Free convection in a triangle cavity filled with a porous medium saturated with nanofluids with flush mounted heater on the wall. *International Journal of Thermal Sciences*, 50(11): 2141-2153. <https://doi.org/10.1016/j.ijthermalsci.2011.06.005>
- [37] Mliki, B., Abbassi, M.A., Omri, A., Zeghamati, B. (2015). Augmentation of natural convective heat transfer in linearly heated cavity by utilizing nanofluids in the presence of magnetic field and uniform heat generation/absorption. *Powder Technology*, 284: 312-325. <https://doi.org/10.1016/j.powtec.2015.06.068>
- [38] Saeid, N.H., Mohamad, A.A. (2005). Natural convection in a porous cavity with spatial sidewall temperature variation. *International Journal of Numerical Methods for Heat & Fluid Flow*, 15(6): 555-566.
<https://doi.org/10.1108/09615530510601459>
- [39] Hatami, M., Song, D., Jing, D. (2016). Optimization of a circular-wavy cavity filled by nanofluid under the natural convection heat transfer condition. *International Journal of Heat and Mass Transfer*, 98: 758-767.
<https://doi.org/10.1016/j.ijheatmasstransfer.2016.03.063>
- [40] Al-Zamily, A.M.J. (2014). Effect of magnetic field on natural convection in a nanofluid-filled semi-circular enclosure with heat flux source. *Computers & Fluids*, 103: 71-85.
<https://doi.org/10.1016/j.compfluid.2014.07.013>
- [41] Han, C.Y., Chang, S.M. (2011). Hydromagnetic flow with thermal radiation. In *Convection and Conduction Heat Transfer*. IntechOpen.
- [42] Nemati, H., Farhadi, M., Sedighi, K., Ashorynejad, H.R., Fattahi, E.J.S.I. (2012). Magnetic field effects on natural convection flow of nanofluid in a rectangular cavity using the Lattice Boltzmann model. *Scientia Iranica*, 19(2): 303-310.
<https://doi.org/10.1016/j.scient.2012.02.016>
- [43] Ashorynejad, H.R., Shahriari, A. (2018). MHD natural convection of hybrid nanofluid in an open wavy cavity. *Results in Physics*, 9: 440-455.
<https://doi.org/10.1016/j.rinp.2018.02.045>
- [44] Mejri, I., Mahmoudi, A., Abbassi, M.A., Omri, A. (2016). LBM simulation of natural convection in an inclined triangular cavity filled with water. *Alexandria Engineering Journal*, 55(2): 1385-1394.
<https://doi.org/10.1016/j.aej.2016.03.020>
- [45] Sheikholeslami, M., Gorji-Bandpy, M., Vajravelu, K. (2015). Lattice Boltzmann simulation of magnetohydrodynamic natural convection heat transfer of Al₂O₃-water nanofluid in a horizontal cylindrical enclosure with an inner triangular cylinder. *International Journal of Heat and Mass Transfer*, 80: 16-25.
<https://doi.org/10.1016/j.ijheatmasstransfer.2014.08.090>
- [46] Hatami, M. (2017). Numerical study of nanofluids natural convection in a rectangular cavity including heated fins. *Journal of Molecular Liquids*, 233: 1-8.
<https://doi.org/10.1016/j.molliq.2017.02.112>
- [47] Ghoben, Z.K., Hussein, A.K. (2023). Three-dimensional analysis of the thermal behavior of alumina-water nanofluid inside hexagonal and octagonal enclosed domain. *Journal of Advanced Research in Fluid Mechanics and Thermal Sciences*, 103(1): 40-63.
<https://doi.org/10.37934/arfmts.103.1.4063>
- [48] Ghoben, Z.K., Hussein, A.K. (2022). Natural convection inside a 3D regular shape enclosures-A brief review. *International Journal of Heat and Technology*, 40: 232-246. <https://doi.org/10.18280/ijht.400128>
- [49] Walker, K.L., Homsy, G.M. (1978). Convection in a porous cavity. *Journal of Fluid Mechanics*, 87(3): 449-474. <https://doi.org/10.1017/S0022112078001718>
- [50] Keramat, F., Dehghan, P., Mofarahi, M., Lee, C.H. (2020). Numerical analysis of natural convection of alumina-water nanofluid in H-shaped enclosure with a V-shaped baffle. *Journal of The Taiwan Institute of Chemical Engineers*, 111: 63-72.
<https://doi.org/10.1016/j.jtice.2020.04.006>
- [51] Keramat, F., Azari, A., Rahideh, H., Abbasi, M. (2020). A CFD parametric analysis of natural convection in an H-shaped cavity with two-sided inclined porous fins. *Journal of The Taiwan Institute of Chemical Engineers*, 114: 142-152.
<https://doi.org/10.1016/j.jtice.2020.09.011>
- [52] Loukili, M., Kotrasova, K., Dutykh, D. (2020). A Computational simulation of steady natural convection in an H-form cavity. *Software Engineering Perspectives in Intelligent Systems. CoMeSySo 2020. Advances in Intelligent Systems and Computing*, vol 1295. Springer, Cham. https://doi.org/10.1007/978-3-030-63319-6_15
- [53] Nadeem, S., Hamed, Y.S., Riaz, M.B., Ullah, I., Alzabut, J. (2024). Finite element method for natural convection flow of Casson hybrid (Al₂O₃-Cu/water) nanofluid inside H-shaped enclosure. *AIP Advances*, 14(8).
<https://doi.org/10.1063/5.0218934>

- [54] Rahimi, A., Sepehr, M., Lariche, M.J., Mesbah, M., Kasaeipoor, A., Malekshah, E.H. (2018). Analysis of natural convection in nanofluid-filled H-shaped cavity by entropy generation and heatline visualization using lattice Boltzmann method. *Physica E: Low-Dimensional Systems and Nanostructures*, 97: 347-362. <https://doi.org/10.1016/j.physe.2017.12.003>
- [55] Eshaghi, S., Izadpanah, F., Dogonchi, A.S., Chamkha, A.J., Hamida, M.B.B., Alhumade, H. (2021). The optimum double diffusive natural convection heat transfer in H-shaped cavity with a baffle inside and a corrugated wall. *Case Studies in Thermal Engineering*, 28: 101541. <https://doi.org/10.1016/j.csite.2021.101541>
- [56] Saleem, K.B., Marafie, A.H., Al-Farhany, K., Hussam, W.K., Sheard, G.J. (2023). Natural convection heat transfer in a nanofluid filled l-shaped enclosure with time-periodic temperature boundary and magnetic field. *Alexandria Engineering Journal*, 69: 177-191. <https://doi.org/10.1016/j.aej.2022.12.030>
- [57] Suchana, K., Islam, M.M., Molla, M.M. (2024). Lattice Boltzmann simulation of cross diffusion via Soret and Dufour effects on natural convection of experimental data-based MWCNTs-H₂O nanofluids in an L-shaped enclosure. *International Journal of Thermofluids*, 21: 100546. <https://doi.org/10.1016/j.ijft.2023.100546>
- [58] Nia, S.N., Rabiei, F., Rashidi, M.M., Kwang, T.M. (2020). Lattice Boltzmann simulation of natural convection heat transfer of a nanofluid in an L-shaped enclosure with a baffle. *Results in Physics*, 19: 103413. <https://doi.org/10.1016/j.rinp.2020.103413>
- [59] Ghalambaz, M., Hashem Zadeh, S.M., Veismoradi, A., Sheremet, M.A., Pop, I. (2021). Free convection heat transfer and entropy generation in an odd-shaped cavity filled with a Cu-Al₂O₃ hybrid nanofluid. *Symmetry*, 13(1): 122. <https://doi.org/10.3390/sym13010122>
- [60] Mahmoodi, M. (2011). Numerical simulation of free convection of a nanofluid in L-shaped cavities. *International Journal of Thermal Sciences*, 50(9): 1731-1740. <https://doi.org/10.1016/j.ijthermalsci.2011.04.009>
- [61] Rahman, M.M., Chamkha, A.J., Elmasry, Y., Ullah, I., Pasha, A.A., Sadeghi, M.S., Galal, A.M. (2022). The heat transfer behavior of MHD micro-polar MWCNT-Fe₃O₄/water hybrid nanofluid in an inclined \perp -shaped cavity with semi-circular heat source inside. *Case Studies in Thermal Engineering*, 38: 102316. <https://doi.org/10.1016/j.csite.2022.102316>
- [62] Almeshaal, M.A., Kalidasan, K., Askri, F., Velkennedy, R., Alsagri, A.S., Kolsi, L. (2020). Three-dimensional analysis on natural convection inside a T-shaped cavity with water-based CNT-aluminum oxide hybrid nanofluid. *Journal of Thermal Analysis and Calorimetry*, 139: 2089-2098. <https://doi.org/10.1007/s10973-019-08533-w>
- [63] Abu-Libdeh, N., Redouane, F., Aissa, A., Mebarek-Oudina, F., Almuhtady, A., Jamshed, W., Al-Kouz, W. (2021). Hydrothermal and entropy investigation of Ag/MgO/H₂O hybrid nanofluid natural convection in a novel shape of porous cavity. *Applied Sciences*, 11(4): 1722. <https://doi.org/10.3390/app11041722>
- [64] Nabwey, H.A., Rashad, A.M., Khan, W.A., Alshber, S.I. (2022). Effectiveness of magnetized flow on nanofluid via unsteady natural convection inside an inclined U-shaped cavity with discrete heating. *Alexandria Engineering Journal*, 61(11): 8653-8666. <https://doi.org/10.1016/j.aej.2022.02.010>
- [65] Ali, F.H., Hamzah, H.K., Egab, K., Arıcı, M., Shahsavari, A. (2020). Non-Newtonian nanofluid natural convection in a U-shaped cavity under magnetic field. *International Journal of Mechanical Sciences*, 186: 105887. <https://doi.org/10.1016/j.ijmecsci.2020.105887>
- [66] Zaim, A., Aissa, A., Mebarek-Oudina, F., Mahanthesh, B., Lorenzini, G., Sahnoun, M., El Ganaoui, M. (2020). Galerkin finite element analysis of magneto-hydrodynamic natural convection of Cu-water nanofluid in a baffled U-shaped enclosure. *Propulsion and Power Research*, 9(4): 383-393. <https://doi.org/10.1016/j.jprr.2020.10.002>
- [67] Ma, Y., Mohebbi, R., Rashidi, M.M., Yang, Z. (2018). Simulation of nanofluid natural convection in a U-shaped cavity equipped by a heating obstacle: Effect of cavity's aspect ratio. *Journal of the Taiwan Institute of Chemical Engineers*, 93: 263-276. <https://doi.org/10.1016/j.jtice.2018.07.026>
- [68] Bagheri, H., Behrang, M., Assareh, E., Izadi, M., Sheremet, M.A. (2019). Free convection of hybrid nanofluids in a C-shaped chamber under variable heat flux and magnetic field: simulation, sensitivity analysis, and artificial neural networks. *Energies*, 12(14): 2807. <http://doi.org/10.3390/en12142807>
- [69] Raizah, Z.A., Ahmed, S.E., Aly, A.M. (2020). ISPH simulations of natural convection flow in E-enclosure filled with a nanofluid including homogeneous/heterogeneous porous media and solid particles. *International Journal of Heat and Mass Transfer*, 160: 120153. <https://doi.org/10.1016/j.ijheatmasstransfer.2020.120153>
- [70] Sannad, M., Btissam, A., Lahoucine, B. (2020). Numerical simulation of the natural convection with presence of the nanofluids in cubical cavity. *Mathematical Problems in Engineering*, 2020(1): 8375405. <https://doi.org/10.1155/2020/8375405>

NOMENCLATURE

B	dimensionless heat source length
CP	specific heat, J. kg ⁻¹ . K ⁻¹
g	gravitational acceleration, m.s ⁻²
k	thermal conductivity, W.m ⁻¹ . K ⁻¹
Nu	local Nusselt number
Ha	Hartmann number
h	the partition's height, m
P	Pressure, N/m ²
Pr	Prandtl number
Ra	Rayleigh number
T	Temperature, k
t	Time, s
u	the x-direction velocity component, m/s
v	the y-direction velocity component, m/s
w	the z-direction velocity component, m/s
x	the coordinate's horizontal component, m
y	the coordinate's vertical component, m
z	the axial direction coordinate, m
AR	Aspect ratio
Da	Darcy numbers

Greek symbols

α	thermal diffusivity, $m^2 \cdot s^{-1}$
β	thermal expansion coefficient, K^{-1}
φ	solid volume fraction
μ	dynamic viscosity, $kg \cdot m^{-1}s^{-1}$
ρ	Density (Kg/m^3)
θ	Cavity's inclination angle ($^\circ$)
ϕ	Side wall Inclination angle ($^\circ$)

Abbreviations

CFD	Computational Fluid Dynamic
CVM	Control Volume Method
FDM	Finite Difference Method
FEM	Finite Element Method
FVM	Finite Volume Method
LBM	Lattice Boltzmann Method
MRT	Multiple Relaxation Time

PIV	Particle Image Velocimetry
Rd	Radiation number
2D	Two-dimensional
3D	Three-dimensional
MHD	Magnetohydrodynamics
TEG	Total Entropy Generation

Subscripts

b	Block
c	Cold
E	External
eff	Effective
f	Fluid
I	Internal
L	Length
hnf	Hybrid Nano fluid
nf	Nano fluid
s	Solid particle